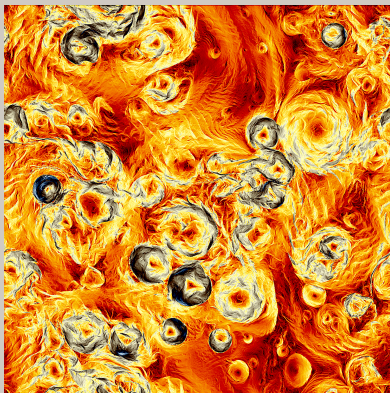


Reflection-driven turbulence in the super-Alfvénic solar wind



Meyrand Romain



UNIVERSITY
of
OTAGO
Te Whare Wānanga o Ōtago
NEW ZEALAND

Reflection-driven turbulence

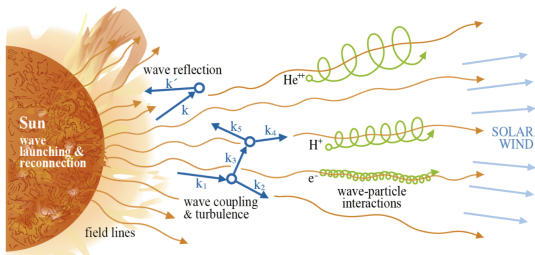


Figure: Image courtesy of B. Chandran

- The Sun launches Alfvén waves, which transport energy outwards
- The waves become turbulent due to wave reflections
- This causes energy to “cascade”, heating the plasma
- This increases the thermal pressure, which then accelerates the solar wind.

Expanding Box Model

We consider the turbulence dynamics in a frame co-moving with a spherically expanding flow.

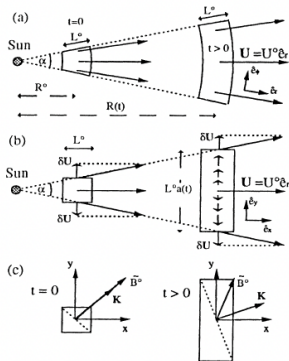


Figure: Grappin et al. 1993

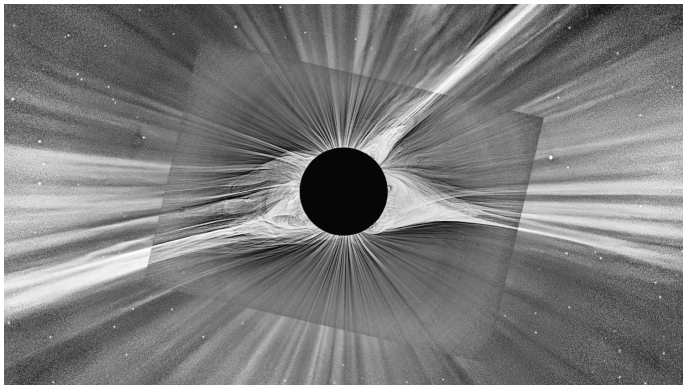
Simplest model imaginable:

- Fluctuations are transverse, non compressible
- Radial background magnetic field
- $k_{\perp} \rho_i \ll 1$
- U is radial, constant and $\gg V_A$
- All fields are 3D periodic

Expanding Box Model

'zeroth-order' questions:

- How fast various types of energy decay?
- How the outer scale evolves?



RMHD Expanding Box Model

$$\dot{a} \frac{\partial \tilde{\mathbf{z}}^{\pm}}{\partial a} \mp \frac{v_{A0}}{a} \frac{\partial \tilde{\mathbf{z}}^{\pm}}{\partial z} + \frac{1}{a^{3/2}} \left(\tilde{\mathbf{z}}^{\mp} \cdot \nabla_{\perp} \tilde{\mathbf{z}}^{\pm} + \frac{\nabla_{\perp} \rho}{\rho} \right) = -\frac{\dot{a}}{2a} \tilde{\mathbf{z}}^{\mp}$$

$$a(t) = \frac{R(t)}{R_0} = 1 + \dot{a}t, \quad \tilde{\mathbf{z}}^{\pm} \doteq a^{1/2} \mathbf{z}_{\perp}^{\pm} \propto \frac{\mathbf{z}_{\perp}^{\pm}}{\sqrt{\omega_A}}$$

RMHD equations with two modifications :

- additional linear terms coupling counter-propagating Alfvénic perturbations: $-\frac{\dot{a}}{2a} \tilde{\mathbf{z}}^{\mp}$
- modified expression for the gradients accounting for the increasing lateral stretching of the plasma with distance: $\nabla_{\perp} \rightarrow \nabla_{\perp}/a$

Characteristic times scales

$$\dot{a} \frac{\partial \tilde{\mathbf{z}}^{\pm}}{\partial a} \mp \frac{v_{A0}}{a} \frac{\partial \tilde{\mathbf{z}}^{\pm}}{\partial z} + \frac{1}{a^{3/2}} \left(\tilde{\mathbf{z}}^{\mp} \cdot \nabla_{\perp} \tilde{\mathbf{z}}^{\pm} + \frac{\nabla_{\perp} \rho}{\rho} \right) = -\frac{\dot{a}}{2a} \tilde{\mathbf{z}}^{\mp}$$

- $\chi_A = \frac{\text{Alfvénic}}{\text{nonlinear}}$
- $\chi_{\text{exp}} = \frac{\text{expansion}}{\text{nonlinear}}$
- $\Delta = \frac{\text{expansion}}{\text{Alfvénic}} = \frac{\chi_{\text{exp}}}{\chi_A} = \text{const.}$

χ_A and χ_{exp} vary during the expansion and their relative values delimit different regimes through which the turbulence evolves during its radial transport.

Basic evolution

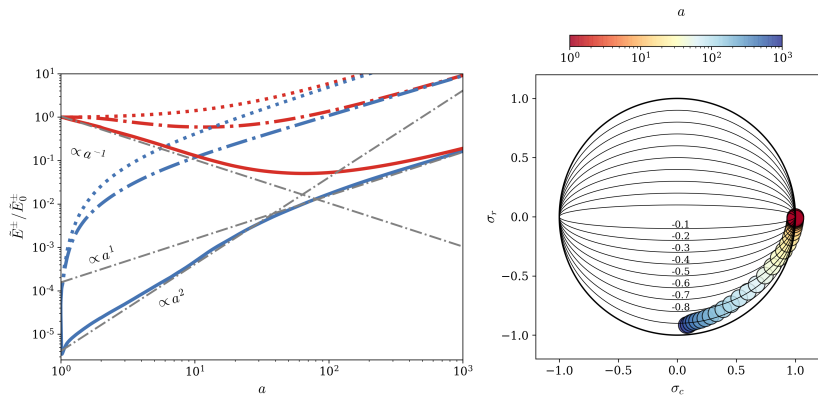
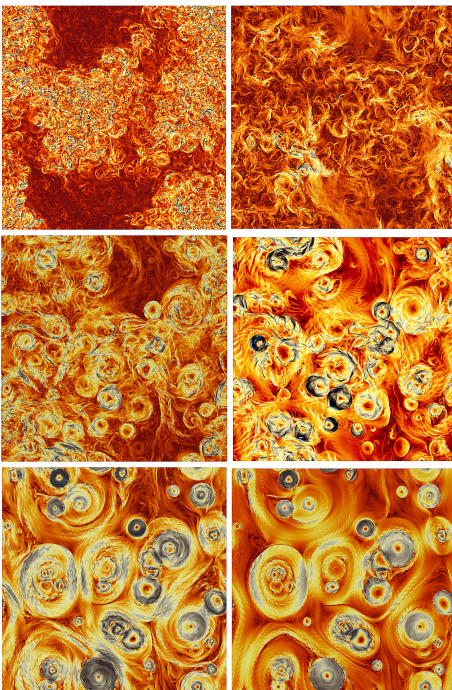


Figure: Left panel: Radial evolution of wave action energies \tilde{E}^+ (red lines) and \tilde{E}^- (blue lines) for three simulations with different amplitude initial conditions. Right panel: Parametric representation of σ_r and σ_c during the evolution. The colors (on a logarithmic scale) indicate the normalized radial distance a . Solid lines represent contours of constant σ_θ .



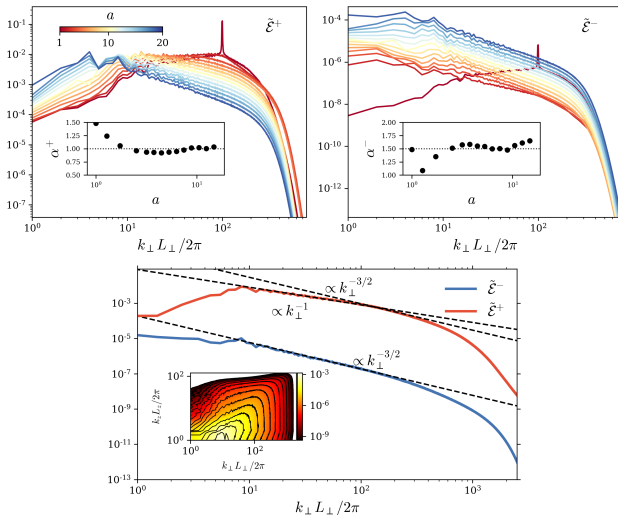


Figure: Wave-action energy spectra $\tilde{\mathcal{E}}^\pm(k_\perp)$ during the imbalanced phase of the simulation. The different colors show different time/radii, as indicated by the color bar. In each panel, the inset shows the best-fit power-law spectral slope.

Turbulent decay phenomenology

$$\dot{a} \frac{\partial \tilde{E}^{\pm}}{\partial a} \sim -\frac{1}{a^{3/2}} \frac{\tilde{E}^{\pm}}{\tau^{\mp}} - \frac{\dot{a}}{a} \tilde{E}^r$$

- Because $\tilde{E}^+ \gg \tilde{E}^r$ when $\tilde{E}^+ \gg \tilde{E}^-$, \tilde{z}^+ is decaying, while \tilde{z}^- is forced by reflection and damped by turbulence.
- The \tilde{z}^- fluctuations remain “anomalously coherent” with the \tilde{z}^+ , because their forcing via reflection is highly coherent ($\propto -\tilde{z}^+$) thus “dragging” \tilde{z}^- along with the \tilde{z}^+ in time.
- The turbulent decay time τ^{\pm} of \tilde{z}^{\pm} is strong for both field:

$$\tau_{\mp}^{-1} \sim a^{-3/2} \frac{\tilde{z}^{\pm}}{\tilde{\lambda}^{\pm}}$$

Turbulent decay phenomenology

$$\dot{a} \frac{\partial \tilde{E}^\pm}{\partial a} \sim -\frac{1}{a^{3/2}} \frac{\tilde{E}^\pm}{\tau^\mp} - \frac{\dot{a}}{a} \tilde{E}^r$$

- $\dot{a} \frac{\partial \tilde{E}^+}{\partial a} \sim -\frac{1}{a^{3/2}} \frac{\tilde{z}^-}{\tilde{\lambda}^-} \tilde{E}^+$
- $\frac{1}{a^{3/2}} \frac{\tilde{z}^+}{\tilde{\lambda}^+} \tilde{E}^- \sim \frac{\dot{a}}{a} |\tilde{E}^r| \sim \frac{\dot{a}}{a} |\sigma_\theta| \tilde{z}^+ \tilde{z}^-, \quad \tilde{z}^- \sim \dot{a} a^{1/2} \tilde{\lambda}^+ |\sigma_\theta|$

$$\sigma_\theta \doteq \frac{\langle \tilde{\mathbf{z}}^+ \cdot \tilde{\mathbf{z}}^- \rangle}{\langle |\tilde{\mathbf{z}}^+|^2 \rangle^{1/2} \langle |\tilde{\mathbf{z}}^-|^2 \rangle^{1/2}} = \frac{\sigma_r}{\sqrt{1 - \sigma_c^2}},$$

$$\sigma_c \doteq \frac{\tilde{E}^+ - \tilde{E}^-}{\tilde{E}^+ + \tilde{E}^-} = \frac{\tilde{E}^c}{\tilde{E}}$$

$$\sigma_r \doteq \frac{\tilde{E}^u - \tilde{E}^b}{\tilde{E}^u + \tilde{E}^b} = \frac{\tilde{E}^r}{\tilde{E}}$$

Turbulent decay phenomenology

- $\dot{a} \frac{\partial \tilde{E}^+}{\partial a} \sim -\frac{1}{a^{3/2}} \frac{\tilde{z}^-}{\tilde{\lambda}^-} \tilde{E}^+$
- $\tilde{z}^- \sim \dot{a} a^{1/2} \tilde{\lambda}^+ |\sigma_\theta| \Rightarrow \tilde{z}^- \sim \tilde{z}^+ / \chi_{\text{exp}}$

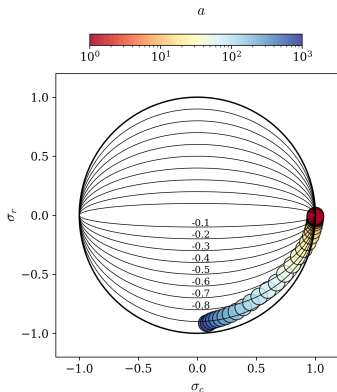
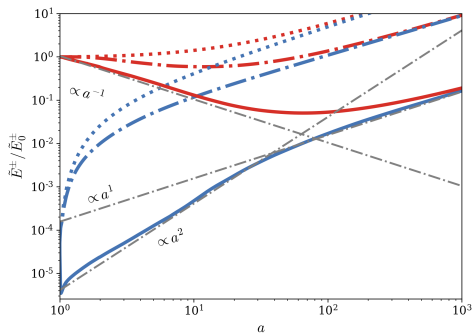
$$\boxed{\frac{\partial \ln \tilde{E}^+}{\partial a} \sim -\frac{1}{a} \frac{\tilde{\lambda}^+}{\tilde{\lambda}^-} \sigma_\theta}$$

The anomalous coherence will break down once \tilde{z}^- enters the weak regime (in which case \tilde{z}^- can propagate away from the source). The phenomenology thus requires

$$\chi_A \doteq \frac{(\tau_-)^{-1}}{v_A / \ell_{\parallel}} \sim \frac{\tilde{z}^+ / \tilde{\lambda}^+}{a^{1/2} v_{A0} / \ell_{\parallel}} \gtrsim 1$$

The phenomenology can only be valid for sufficiently large-amplitude \tilde{z}^+ with $\chi_{\text{exp}} \gg 1$ irrespective of the fluctuation's parallel scale, and we expect the transition to the balanced regime to occur when \tilde{E}^+ decays sufficiently so that $\chi_{\text{exp}} \sim 1$.

Basic evolution



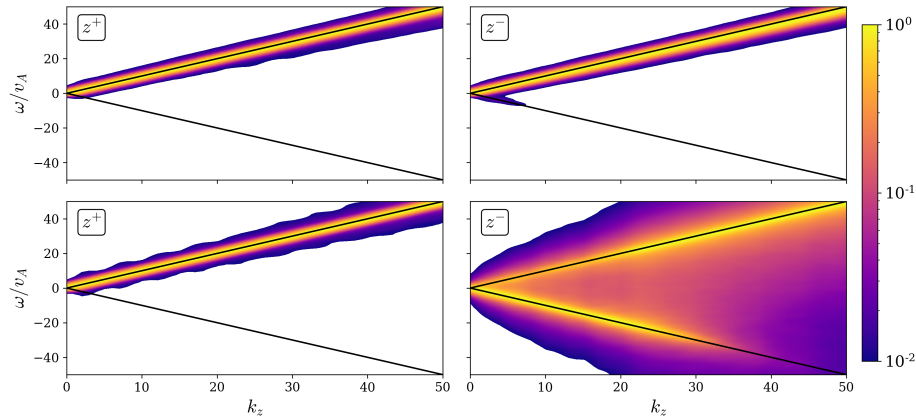
$$\sigma_{\theta} \tilde{\lambda}^{+} / \tilde{\lambda}^{-} \approx 1 \Rightarrow \tilde{E}^{+} \propto a^{-1}$$

$$\sigma_{\theta} \tilde{\lambda}^{+} \propto a^{1/2}$$

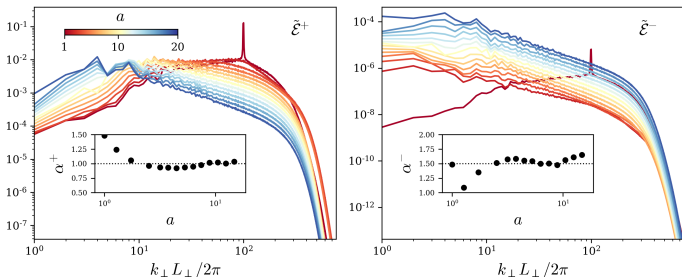
Anomalous coherence

Space-time Fourier spectrum:

$$\tilde{\mathcal{E}}^{\pm}(k_z, \omega) = \frac{1}{2} \left\langle |\hat{\mathbf{z}}^{\pm}(k_z, \omega)|^2 \right\rangle_{\perp}$$



The growth of \tilde{L}_+



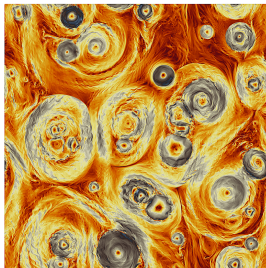
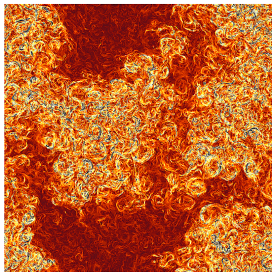
- $\tilde{\mathcal{E}}^+(k_{\perp})$ migrate towards large scales during the expansion. As this occurs, $\tilde{\mathcal{E}}^+$ develops a wide $\tilde{\mathcal{E}}^+ \propto k_{\perp}^{-1}$ range.
- The evolution of $\tilde{\mathcal{E}}^-(k_{\perp})$ is quite different, rapidly moving to large scales at very early times.

Anomalous conservation of anastrophy

In the nonlinear regime, the weaker field is born coherent and is short-lived. It doesn't propagate against but with the stronger field. The dynamic is effectively 2D like which suggest that anastrophy $\langle A_z^2 \rangle$ is anomalously conserved.

$$\langle A_z^2 \rangle \sim a^{-1} \tilde{E}^+ \tilde{L}_+^2 \sim \text{const.} \implies \tilde{L}_+ \propto a$$

The turbulent decay must progress with \tilde{L}_+ increasing rapidly in time.



Anomalous conservation of anastrophy

We compute the parametric representation,

$$X(a) = -\frac{\partial \ln \tilde{z}_{\text{rms}}^+(a)}{\partial \ln a}, \quad Y(a) = \frac{\partial \ln \tilde{L}_+(a)}{\partial \ln a},$$

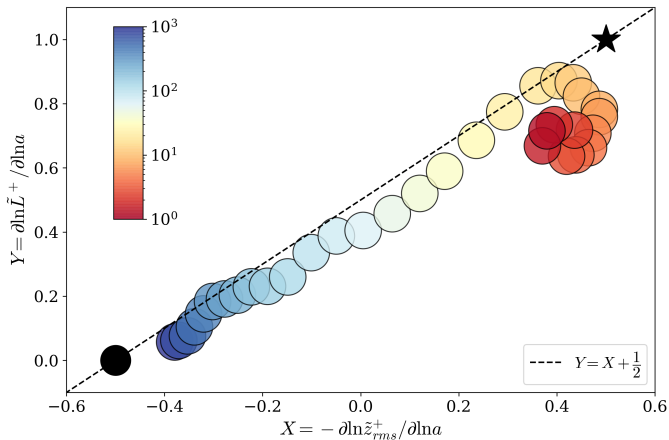
where $\tilde{z}_{\text{rms}}^+ = \sqrt{2\tilde{E}^+}$ and \tilde{L}_+ is computed as

$$\tilde{L}_+ \equiv \int dk_{\perp} \tilde{\mathcal{E}}^+(k_{\perp})/k_{\perp}.$$

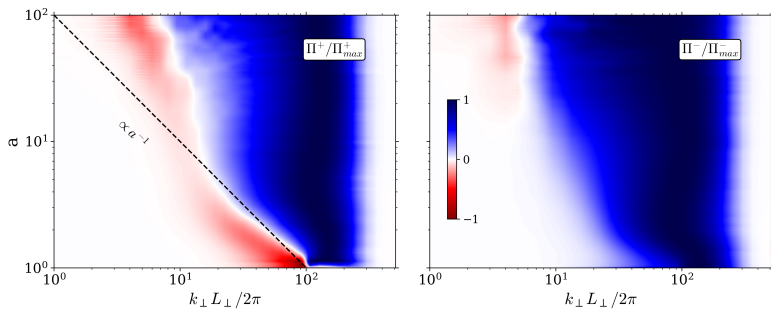
$X(a)$ and $Y(a)$ are the instantaneous scaling exponents of $1/\tilde{z}_{\text{rms}}^+$ and \tilde{L}_+ . If anastrophy is conserved then

$$Y(a) = X(a) + \frac{1}{2}.$$

Anomalous conservation of anastrophy



The split cascade

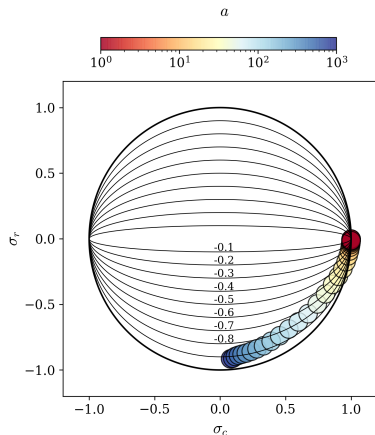
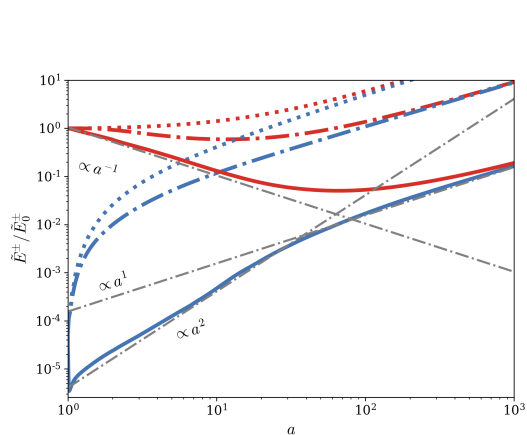


$$\Pi^\pm(k_\perp) = a^{-3/2} \frac{2\pi}{L_\perp} \int \frac{d^3\mathbf{r}}{V} [\tilde{\mathbf{z}}^\pm]_{k_\perp}^< \cdot (\tilde{\mathbf{z}}^\mp \cdot \tilde{\nabla}_\perp \tilde{\mathbf{z}}^\pm),$$

where the low-pass filter is defined by

$$[\tilde{\mathbf{z}}^\pm]_{k_\perp}^< = \sum_{k'_z} \sum_{|\mathbf{k}'_\perp| \leq k_\perp} e^{i\mathbf{k}' \cdot \mathbf{r}} \tilde{\mathbf{z}}_{\mathbf{k}'}^\pm.$$

Balanced, magnetically dominated phase



Linear Dynamics

Eigenmodes

$$\xi^\pm = \frac{1}{2} \tilde{z}_w^\pm \pm i (\Delta \mp \omega^\pm) \tilde{z}_w^\mp$$

$$\omega^\pm = \pm \sqrt{\Delta^2 - 1/4}$$

- For $\Delta > 1/2$, ω^\pm is real and \tilde{z}^\pm oscillates with frequency ω^\pm .
- For $\Delta < 1/2$, ω^\pm is imaginary and modes grow exponentially, $\tilde{z}^\pm \propto e^{|\omega^\pm| \ln a} = a^{|\omega^\pm|} = a^{\sqrt{1-4\Delta^2}/2}$.

The growing expansion-dominated mode, with $\omega = i\sqrt{1/4 - \Delta^2}$, is magnetically dominated with $\tilde{\mathbf{z}}^- \approx -\tilde{\mathbf{z}}^+$ and $|\tilde{\mathbf{b}}_\perp| \gg |\tilde{\mathbf{u}}_\perp|$

Linear Dynamics

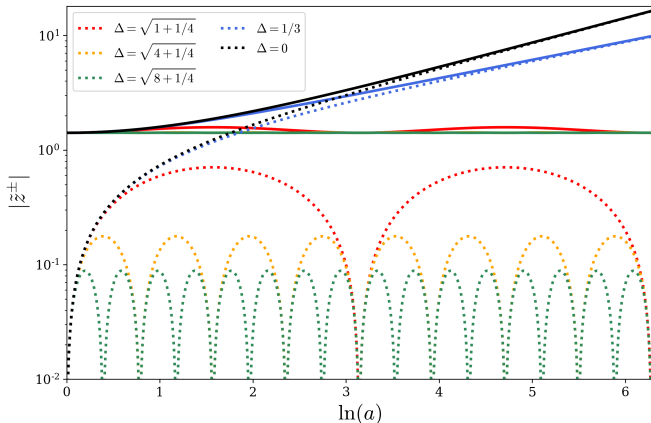


Figure: Solutions of the linearised equations, starting from the initial condition $\tilde{z}^-(0) = 0$ and $\tilde{z}^+(0) = \sqrt{2}$ with different values of Δ as labelled. Solid lines show $|\tilde{z}^+(a)|$; dotted lines show $|\tilde{z}^-(a)|$.

Emergence of Alfvén vortices

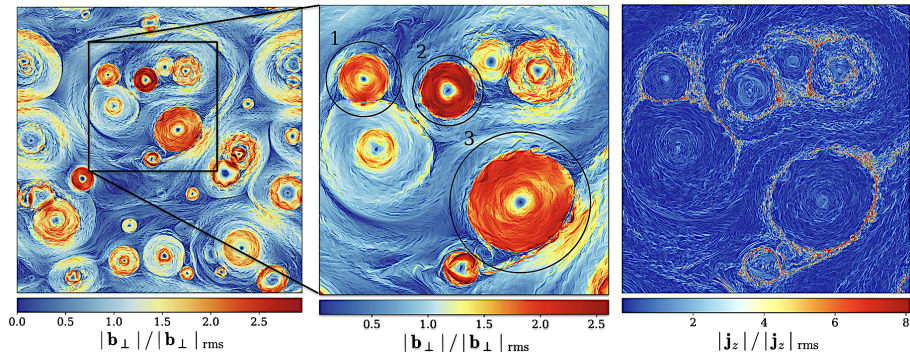


Figure: Left: Snapshot of the magnetic field modulus in a plane perpendicular to B_0 at $a = 250$. Middle: Close-up corresponding to the marked region on the left, illustrating Alfvén vortices colliding and merging through reconnection. Right: Same region as the middle panel, but showing the out-of-plane current.

Emergence of Alfvén vortices

We start from the variational problem

$$\delta \int d^3\mathbf{r} \left(|\tilde{\nabla}_{\perp} \tilde{A}_z|^2 - \Lambda \tilde{A}_z^2 \right) = 0,$$

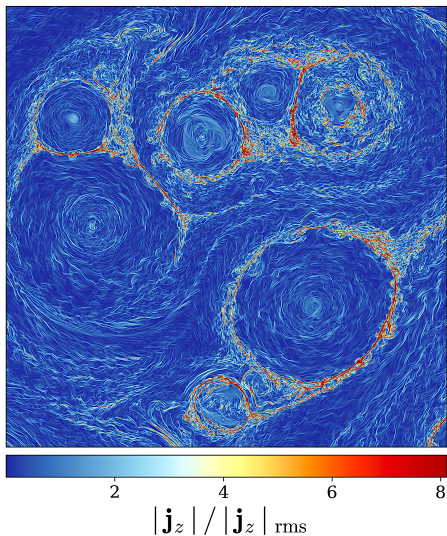
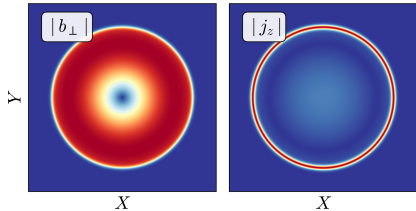
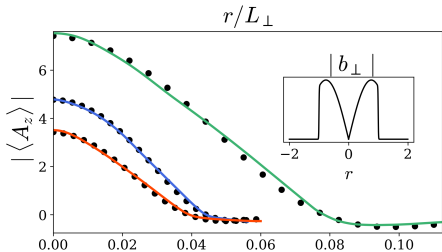
where δ denotes the functional derivative and Λ a Lagrangian multiplier. Identifying Λ with a characteristic scale K_{\perp} via $\Lambda = -K_{\perp}^2$, the Euler-Lagrange equation becomes the Helmholtz equation.

$$\tilde{\nabla}_{\perp}^2 \tilde{A}_z = -K_{\perp}^2 \tilde{A}_z.$$

$$\begin{cases} \tilde{A}_z(r) = A_0 J_0(K_{\perp} r), & r < r_c \\ \tilde{A}_z(r) = A_B, & r \geq r_c \end{cases}$$

The solution corresponds to a particular case of so-called Alfvén vortex solutions, the vortex monopole. The equilibrium is effectively a screw pinch, with its nonlinear equilibrium resulting from the balance between the curvature/tension force and the pressure gradient.

Emergence of Alfvén vortices



Conclusions

In its simplest form, the reflection-driven turbulence may explain essential features of the solar wind:

- Double power law at intermediate and large scales, with power indices $-3/2$ and -1 respectively
- Bi-directional Elsasser cascades in highly imbalance streams.
- Formation of Alfvén vortices.
- Generation of high negative residual energy states.

Thank you for your attention



Figure: Courtesy of Maxwell Busby